NASA Technical Memorandum 106600

17P

Laminated Thin Shell Structures Subjected to Free Vibration in a Hygrothermal Environment

Pascal K. Gotsis and James D. Guptill
Lewis Research Center
Cleveland, Ohio

JULY 1994

National Aeronautics and
Space Administration

LAMINATED THIN SHELL STRUCTURES SUBJECTED TO FREE VIBRATION IN A HYGROTHERMAL ENVIRONMENT

Pascal K. Gotsis and James D. Guptill
National Aeronautics and Space Administration
Lewis Research Center
Cleveland, Ohio 44135

SUMMARY

Parametric studies were performed to assess the effects of various parameters on the free-vibration behavior (natural frequencies) of $[\pm\theta]_2$ angle-ply, fiber composite, thin shell structures in a hygrothermal environment. Knowledge of the natural frequencies of structures is important in considering their response to various kinds of excitation, especially when structures and force systems are complex and when excitations are not periodic. The three-dimensional, finite element structural analysis computer code CSTEM was used in the Cray YMP computer environment. The fiber composite shell was assumed to be cylindrical and made from T300 graphite fibers embedded in an intermediate-modulus, high-strength matrix. The following parameters were investigated: the length and the laminate thickness of the shell, the fiber orientation, the fiber volume fraction, the temperature profile through the thickness of the laminate, and laminates with different ply thicknesses. The results indicate that the fiber orientation and the length of the laminated shell had significant effects on the natural frequencies. The fiber volume fraction, the laminate thickness, and the temperature profile through the shell thickness had weak effects on the natural frequencies. Finally, the laminates with different ply thicknesses had an insignificant influence on the behavior of the vibrated laminated shell. Also, a single through-the-thickness, eight-node, three-dimensional composite finite element analysis appears to be sufficient for investigating the free-vibration behavior of thin, composite, angle-ply shell structures.

INTRODUCTION

High-speed flight vehicles require new materials able to withstand hostile environments (moisture and temperature) at speeds that are a multiple of the speed of sound and improved computational approaches to designing them. The new materials, known as elevated-temperature composites, have high strength, are light in weight, and can be tailored for the required performance. These materials are already finding applications and acceptance in aircraft frame and engine structures. Cost-effective usage of elevated-temperature composite materials requires new ideas and innovative concepts in material selection and structure fabrication in order to design them for durability by properly accounting for the many failure mechanisms inherent in composites. The influence of hostile environments, nonlinear material, and structural behavior and the coupling between responses induced by various loads require sophisticated analysis methods.

A stand-alone, multidisciplinary computer code, CSTEM (Coupled Structural, Thermal, and Electromagnetic Analysis and Tailoring) (refs. 1 to 7), has been developed by integrating three-dimensional, finite element, structural and stress analysis methods with several single-discipline codes including those for integrated composite mechanics (refs. 8 and 9). The advantage of performing finite element analysis using three-dimensional brick elements is that the temperature gradient as well as the stress gradient can be varied through the thickness of the laminated structure, in contrast to two-dimensional plate elements.

This report presents parametric studies that used the CSTEM computer code to assess the effects of various parameters on an aircraft engine composite shell structure subjected to free vibration at elevated temperatures. Knowledge of the natural frequencies of structures is important in considering their response to various kinds of excitation, especially when structures and force systems are complex and when excitations are not periodic

(refs. 10 and 11). The structure studied is a thin, cylindrical composite shell. The composite is to be made from $[\pm\theta]_2$ angle-ply laminates containing plies with uniform thickness. Parametric studies were performed to examine the effects on the natural frequencies of parameters, such as the length and laminate thickness of the shell, the temperature profile through the thickness of the laminate, the fiber volume fraction, the fiber orientation, and laminates with different ply thicknesses.

BRIEF DESCRIPTION OF SIMULATION PROCEDURE

The general-purpose computer code CSTEM (ref. 4) computationally simulates the coupled multidisciplinary structural, heat transfer, vibration, acoustic, and electromagnetic behavior of elevated-temperature, layered, multimaterial composite structures. All the disciplines are coupled for nonlinear geometrical, material, loading, and environmental effects. CSTEM is based on a modular structure (fig. 1) and is accessed by the user through its executive module. The structural response can be predicted at all the composite scales including constituent (fiber and matrix) and ply level.

The composite mechanics is simulated with the ICAN (Integrated Composite Analyzer) module (refs. 8 and 9), which performs, among others, through-the-thickness point stress analysis. The micromechanics equations embedded in ICAN include the effects of temperature and moisture. ICAN simulates the behavior of polymer composites from the constituent material level to the laminate level, as depicted in figures 2 and 3. ICAN includes a resident material property data bank for commercially available fiber and matrix constituent materials at room temperature. The user needs only to specify a code name for the desired constituent materials (rather than having to manually input all the properties) in the CSTEM input.

The procedure for computationally simulating composite structures is shown in figure 2 and consists of four parts: the constituents, the synthesis, the finite element structural analysis, and the decomposition. For a detailed description of these four parts see references 8 and 9. The computational procedure steps are as follows:

(1) Constituents. The material properties of the matrix in any operational temperature and moisture conditions are updated by using the constitutive equation depicted in figure 3. The fiber properties were assumed to be unchanged by the hygrothermal conditions.

(2) Synthesis. The thermal and mechanical properties of the plies are synthesized from the mechanical properties of the fibers and matrix by using composite micromechanics theory. The extensional stiffness matrix A, the coupling stiffness matrix B, and the bending stiffness matrix D are computed by using laminate theory and the thermal and mechanical effective laminate engineering properties (ref. 12).

(3) Finite element analysis. The finite element analysis is performed at the composite structural level, and among others, the resulting forces and moments are computed at each node of the finite element mesh. Because ICAN performs through-the-thickness point stress analysis, steps (1) and (2) and the upcoming step (4) are performed at each individual node of the finite element mesh.

(4) Decomposition. The stresses and strains in each ply are computed by using laminate theory. The stresses and strains within the matrix and the fibers for each ply are computed by using composite micromechanics.

The CSTEM code is written in FORTRAN programming language and is installed on the NASA Lewis Cray YMP computer system.

SUMMARY OF STRUCTURAL EQUATIONS

The equations of equilibrium governing the linear dynamic response of the structure written in matrix form are the following (refs. 10 and 11):

$$[\mathrm{M}]\ddot{U} + [\mathrm{D}]\dot{U} + [\mathrm{K}]U = \{R(t)\} \tag{1}$$

where

[M]	structural mass matrix
[D]	structural damping matrix
[K]	structural stiffness matrix
$\{R(t)\}$	external applied load vector, as a function of time
$\{U\}$	displacement vector
$\{\dot{U}\}$	velocity vector
$\{\ddot{U}\}$	acceleration vector

The equilibrium equations (1), in the case of the free-vibration problem, are simplified by setting the load vector equal to zero, $\{R(t)\} = 0$. If the damping effect is not taken into account, the damping matrix is equal to zero, [D] = 0.

The equilibrium equations are simplified as follows:

$$[\mathrm{M}]\ddot{U} + [\mathrm{K}]U = 0 \tag{2}$$

The structural matrices [M] and [K] are computed by discretizing the continuous structure into a number of finite elements. If [H] is the shape function of a finite element of the structure, then

(1) The mass matrix of the element is given by

$$[\mathrm{m}] = \int_v \rho \{H\}^T \{H\} dV$$

where ρ is the mass density of the element.

(2) The stiffness matrix of the element is given by

$$[\mathrm{k}] = \int_v [B]^T [C] [B] dV$$

where [C] is the material matrix of the element, which contains the anisotropic effective properties of the laminate and is related to the stress-strain relationship by

$$\{\sigma\} = [\mathrm{C}] \{\varepsilon\}$$

The matrix [B] is related to the strain displacement relationship by

$$\{\varepsilon\} = [B]\{u\}$$

where [B] = [L] [N], [L] is a linear operator, and [N] is the matrix that consists of the shape functions [H] (ref. 13).

The structural mass matrix [M] is assembled from the element mass matrices $[m]_j$ for $j = 1, n_{el}$, where n_{el} is the number of finite elements in the structure. Similarly, the structural stiffness matrix [K] is assembled from the element stiffness matrices $[k]_j$, $j = 1, n_{el}$.

After the computation of the [M] and [K] matrices the next step is to solve equation (2). The solution of equation (2) can be postulated to be of the following form:

$$U = \{\phi\} \sin \omega (t - t_0) \tag{3}$$

Substituting equation (3) into equation (2) gives

$$[K]\{\phi\} = \omega^2 [M]\{\phi\} \tag{4}$$

For the computation of the vibration frequencies (eigenvalues) and mode shapes (eigenvectors), CSTEM incorporates the following two methods: the determinant search and the subspace iteration (refs. 11 and 14). The search method is intended more for a small number of equations; the subspace iteration is more efficient for a large number of equations.

GEOMETRY, LOAD HISTORY, AND FINITE ELEMENT MODEL OF LAMINATED SHELLS

The thin composite shell had a cylindrical geometry with the following dimensions: ratio of inner radius to laminate thickness of the shell $R/t = 33.3$; $R = 25.4$ cm; ratio of longitudinal length to radius $L/R = 2$, 4, and 6. The boundary conditions were one end fixed and the other free (fig. 4). The laminate consisted of continuous fibers made of the graphite material T300 embedded in an intermediate-modulus, high-strength (IMHS) matrix. The material properties of the fiber and matrix were taken from the data bank available in CSTEM (tables 1 and 2). The fiber volume fraction (FVR) was 55 percent and the moisture content was 2 percent. A balanced and nonsymmetric laminate was assumed with fiber orientations of $[\pm\theta]_2$ and plies of equal thickness.

The simulation of the processing of the laminated cylinder was taken into account. The glass transition (curing) temperature T_g of the matrix was initially 215.55 °C (table 2) and was gradually reduced until the operating temperature was equal to $T_g/2$ (fig. 4). At the end of the processing, residual stresses were induced in the constituent materials of the composite structure.

For the free-vibration analysis of the shell structure the effect of damping was neglected. The effect of interlaminar shear stresses was taken into account and is described in detail in the CSTEM users manual (ref. 4). The computational simulation was performed by using the three-dimensional, finite element analysis code CSTEM. One element (eight nodes) through the thickness of the composite shell structure was used. The finite element mesh consisted of 760 nodes and 360 elements (fig. 5).

RESULTS AND DISCUSSION

In this section the results obtained for the different $[\pm\theta]_2$ angle-ply composite shells are presented and discussed. The parameters investigated include

(1) Effects of fiber orientation
(2) Effects of shell length
(3) Effects of laminate thickness
(4) Effects of temperature
(5) Effects of fiber volume fraction
(6) Effects of different ply thicknesses

Effects of Shell Length

The influence of shell length in conjunction with ply angle θ was examined to study the free-vibration behavior of the composite shell. Results obtained for natural frequencies and mode shapes are summarized here.

Natural frequencies.—Three thin composite shells with length ratios L/R of 2, 4, and 6 were examined. The computed values of the first natural frequency are plotted versus θ and the three L/R ratios in figure 6. The computed values are normalized with respect to the maximum frequency of 554.9 Hz. Correspondingly, the computed values of the second natural frequency are normalized with respect to the maximum frequency of 609.6 Hz and are plotted in figure 7. Finally, the computed values of the third natural frequency are normalized with respect to the maximum frequency of 871.8 Hz and are shown in figure 8. The following conclusions were reached:

(1) For all L/R the natural frequencies increased for $0° \le \theta \le 22.5°$ and decreased for $22.5° \le \theta \le 90°$. The maximum frequencies (first, second, and third) occurred at $\theta = 22.5°$.

(2) The shorter the shell, the higher the frequencies, as expected because shorter shells are stiffer than longer shells.

(3) The percentage differences of the natural frequencies between the short ($L/R = 2$) and long ($L/R = 6$) shells for the different ply angles are significant (table 3) and depend on the ply angle.

Mode Shapes.—The behaviors of the mode shapes of the composite shell with $L/R = 6$ and $R/t = 33.3$ for the first three frequencies are presented graphically as follows:

(1) First (lowest) frequency: The mode shape (fig. 9) is primarily bending, indicating that the shell behaves like a cantilever beam.

(2) Second frequency: The mode shape (fig. 10) is a combination of torsional and breathing (or radial) modes.

(3) Third frequency: The mode shape (fig. 11) is a combination of torsional, breathing (or radial), and axial (or longitudinal) modes.

These mode shapes are summarized in table 4 for $0° \le \theta \le 90°$.

Effects of Laminate Thickness

The influence of laminate thickness of the thin composite shell versus the ply angle θ for laminate thickness ratios R/t of 20, 33.3, and 100 is presented in figure 12. The computed values are normalized with respect to the maximum frequency of 264.4 Hz. The following conclusions were reached from figure 12:

(1) For all R/t the first natural frequencies increased for $0° \leq \theta \leq 15°$ and decreased for $15° \leq \theta \leq 90°$. The maximum frequency occurred at $\theta = 15°$.

(2) The thicker the composite shell, the higher the values of the natural frequencies. Thus, thick composite shells ($R/t = 20$) had the highest frequencies, and thin composite shells ($R/t = 100$) had the lowest frequencies. The frequencies maximized at $\theta = 15°$.

(3) The percentage difference of the natural frequencies between the thick laminated shell ($R/t = 20$) and the thin laminated shell ($R/t = 100$) was relatively small (table 5).

Therefore, the laminate thickness ratio R/t had only a small effect on the first natural frequencies of the laminated shell.

Effects of Temperature

The effects of temperature and moisture profiles through the laminate thickness on the free vibration in conjunction with ply angle θ were examined. Three temperature profiles with uniform moisture (2 percent) were considered. The first profile was uniform with temperature equal to room temperature (21 °C), the second profile was also uniform with temperature equal to $T_g/2$ (107.7 °C), and the third profile varified linearly, with temperature equal to $T_g/2$ at the inner surface and room temperature at the outer surface of the composite shell. The length ratio L/R was 4 and the laminate thickness ratio R/t was 33.3. The computed values of the first natural frequency, normalized with respect to the maximum value of 276.8 Hz, are plotted versus ply angle θ for three temperature profiles in figure 13. The following observations were made:

(1) For all temperature profiles the natural frequencies increased for $0° \leq \theta \leq 20°$ and decreased for $20° \leq \theta \leq 90°$. The frequency peaked at $\theta = 20°$.

(2) The room-temperature composite shell had the highest frequencies, followed by the composite shell with the linear profile and finally the composite shell with the uniform temperature equal to $T_g/2$.

(3) The percentage difference in natural frequency between the uniform room-temperature profiles and $T_g/2$ was low (table 5) and was almost independent of θ.

Therefore, the temperature profile had little effect on the natural frequencies of the composite shell throughout the angle-ply range.

Effects of Fiber Volume Fraction

The effects of fiber volume fraction in conjunction with ply angle θ on the free-vibration behavior of the composite shell were evaluated. Three fiber volume fractions were examined: 55, 60, and 65 percent. The length ratio L/R was 4 and the laminate thickness ratio R/t was 33.3. The computed values of the first natural

frequency, normalized with respect to the maximum value of 278.6 Hz, are plotted versus ply angle θ for the various fiber volume fractions in figure 14. The following conclusions were reached:

(1) For all fiber volume fractions the natural frequencies increased for $0° \leq \theta \leq 20°$ and decreased for $20° \leq \theta \leq 90°$. The maximum natural frequency occurred at $\theta = 20°$, which was the same for all the cases investigated.

(2) The composite shell with 65-percent fiber volume fraction had higher frequencies than the shell with the 60-percent fiber volume fraction, which had higher frequencies than the shell with 55-percent fiber volume fraction.

(3) The percentage difference in the natural frequencies between the two laminates with fiber volume fractions of 65 and 55 was very low (table 5).

Therefore, the fiber volume fraction had little effect on the natural frequencies of the composite shell.

Effects of Ply Thickness

The effects of laminates with various ply thicknesses in conjunction with ply angle θ on the natural frequencies of the composite shell were examined. The length ratio L/R was 4, the laminate thickness ratio R/t was 33.3, and the fiber volume fraction was 55 percent. Four laminated shells with different ply thicknesses and the same laminate thickness t were examined: (1) a $[\pm\theta]$ angle-ply laminate with equal ply thicknesses ($t/2$, $t/2$), (2) a $[\pm\theta]_2$ angle-ply laminate with nonuniform ply thicknesses ($3t/8$, $t/8$, $t/8$, $3t/8$), (3) a $[\pm\theta]_2$ angle-ply laminate with uniform ply thicknesses ($t/4$, $t/4$, $t/4$, $t/4$), and (4) a $[\pm\theta]_4$ angle-ply laminate with equal ply thicknesses ($t/8$, $t/8$,...,$t/8$). The computed values for the first natural frequencies of these examined laminates are plotted versus θ in figure 15. The following conclusions were reached:

(1) The natural frequencies increased for $0° \leq \theta \leq 20°$, decreased for $20° \leq \theta \leq 90°$, and peaked at $\theta = 20°$.

(2) The laminas with different ply thicknesses had an insignificant effect on the natural frequencies of the thin composite shells.

FINITE ELEMENT ANALYSIS USING EIGHT-NODE, THREE-DIMENSIONAL ELEMENTS VERSUS FOUR-NODE PLATE ELEMENTS

The behaviors of the shell structure subjected to free vibration using eight-node, three-dimensional elements versus four-node plate elements were compared. The geometry of the laminated structure consisted of a cylinder with length equal to 40 in., an inner radius equal to 10 in., and uniform laminate thickness equal to 0.3 in. The laminate consisted of graphite T300 fibers and a high-strength IMHS matrix. The fiber volume fraction was 55 percent, the ply angle was $[0/90]_2$, and the moisture was 2 percent. The laminated structure had an initial temperature of 215.55 °C that was gradually reduced to the operational temperature of 108 °C. The natural frequencies were computed by using the MHOST computer code (ref. 15) in conjunction with plate element 75, normalized, and plotted in figure 16. The frequencies obtained with the eight-node, three-dimensional elements were higher than the frequencies obtained with the four-node plate elements. The reason is that the eight-node element is stiffer than the plate element and therefore the natural frequencies are higher.

In order to improve the accuracy of the computational simulation of laminated, thin shell structures subjected to free vibration, it is recommended that a 20-node brick element be used or that an eight-node brick element be used and the mesh refined.

SUMMARY OF RESULTS

The free vibration of thin composite shell structures in a hygrothermal environment was computationally simulated by using the CSTEM three-dimensional, finite element analysis computer code. The simulation included the effects of parameters such as ply angle, shell length and laminate thickness, temperature, and fiber volume fraction on the free-vibration behavior of the composite shells. The important results are summarized as follows:

(1) The ply angle and the length of the laminated shell significantly influenced the free-vibration (frequencies and mode shapes) behavior of the composite shells.

(2) The fiber volume fraction, the laminate thickness, and the temperature profile through the laminate thickness had little effect on the free-vibration behavior of the composite shells.

(3) The laminates with different ply thicknesses had an insignificant effect on the free-vibration behavior of the composite shells.

(4) A single through-the-thickness, eight-node, three-dimensional-composite finite element analysis appears to be sufficient for investigating the free-vibration behavior of thin, composite, angle-ply cylindrical shells.

ACKNOWLEDGMENT

The authors would like to thank Dr. Christos C. Chamis for his helpful discussion of the present paper.

REFERENCES

1. Gotsis, P.K.; and Guptill, J.D.: Buckling Analysis of Laminated Thin Shells in a Hot Environment. NASA TM–106302, 1993.

2. Gotsis, P.K.; and Guptill, J.D.: Free Vibration of Fiber Composite Thin Shells in a Hot Environment. Accepted for publication in the Journal of Reinforced Plastic and Composites in April 1994.

3. Gotsis, P.K.; and Guptill, J.D.: Fiber Composite Thin Shells Subjected to Thermal Buckling Loads. Accepted for publication in the International Journal of Computers and Structures in June 1994.

4. Hartle, M. : CSTEM User's Manual. General Electric Company, Cincinnati, OH, 1990.

5. Chamis, C.C.; and Singhal, S.N.: Coupled Multi-Disciplinary Simulation of Composite Engine Structures in Propulsion Environment. NASA TM–105575, 1992.

6. Singhal, S.N.; Murthy, P.L.N.; and Chamis, C.C.: Coupled Multi-Disciplinary Composites Behavior Simulation. NASA TM–106011, 1993.

7. Singhal, S.N., et al.: Computational Simulation of Acoustic Fatigue for Hot Composite Structures. NASA TM–104379, 1991.

8. Murthy, P.L.N.; and Chamis, C.C.: Integrated Composite Analyzer (ICAN)—User's and Programmer's Manual. NASA TP–2515, 1986.

9. Chamis, C.C.: Simplified Composite Micromechanics Equations for Hygral, Thermal, and Mechanical Properties. NASA TM–83320, 1987.

10. Hurty, W.C.; and Rubinstein, M.F.: Dynamics of Structures. Prentice-Hall, Inc., 1964.

11. Meirovitch, L.: Analytical Methods in Vibrations. MacMillan Company, 1967.

12. Whitney, J.M.; Daniel, I.M.; and Pipes, R.B.: Experimental Mechanics of Fiber Reinforced Composite Materials. The Society for Experimental Mechanics, Brookfield Center, CT, 1984.

13. Zienkiewicz, O.C.: The Finite Element Method. Third ed. McGraw-Hill Co., 1977.

14. Bathe, K.J.: Finite Element Procedures in Engineering Analysis. Prentice-Hall, 1982.

15. Nakazawa, S.: The MHOST Finite Element Program: 3–D Inelastic Analysis Methods for Hot Section Components, Volume I. Theoretical Manual. NASA CR–182205, 1991.

TABLE 1.—T300 GRAPHITE FIBER PROPERTIES

AT ROOM TEMPERATURE

Modulus in longitudinal direction, GPa	220.7
Modulus in transverse direction, GPa	13.79
In-plane Poisson's ratio	0.20
Out-of-plane Poisson's ratio	0.25
In-plane shear modulus, GPa	8.96
Out-of-plane shear modulus, GPa	4.827
Thermal expansion coefficients in longitudinal direction, 10^{-6} mm/(mm-°C)	0.99
Thermal expansion coefficients in transverse direction, 10^{-6} mm/(mm-°C)	10.00
Thermal conductivity in longitudinal direction, W/(m-K)	83.69
Thermal conductivity in transverse direction, W/(m-K)	8.369
Fiber tensile strength, GPa	2.413
Fiber compressive strength, GPa	2.069

TABLE 2.—IMHS MATRIX PROPERTIES

AT ROOM TEMPERATURE

Modulus in longitudinal direction, GPa	3.448
Modulus in transverse direction, GPa	3.448
In-plane Poisson's ratio	0.35
Out-of-plane Poisson's ratio	0.35
Thermal expansion coefficients in longitudinal direction, 10^{-6} mm/(mm-°C)	64.8
Thermal expansion coefficients in transverse direction, 10^{-6} mm/(mm-°C)	64.8
Thermal conductivity in longitudinal direction, W/(m-K)	2.16
Thermal conductivity in transverse direction, W/(m-K)	2.16
Matrix tensile strength, MPa	103.4
Matrix compressive strength, MPa	241.3
Matrix shear strength, MPa	89.6
Void fraction	0.225
Glass transition temperature, °C	215.55

TABLE 3.—PERCENT DIFFERENCE[a] IN NATURAL FREQUENCIES BETWEEN SHORT (L/R = 2) AND LONG (L/R = 6) CYLINDERS

Frequency	$[0]_4$	$[\pm15]_2$	$[\pm30]_2$	$[\pm45]_2$	$[\pm60]_2$	$[\pm75]_2$	$[\pm90]_2$
	Difference in natural freqencies, percent						
First	57	60.7	63.5	70.7	73.3	74.1	75.4
Second	60	59.6	67	65.9	63.5	55.7	40
Third	58	45.4	50	55.4	54.9	57.7	57.3

[a]Percent difference = $\frac{\text{Frequency}(L/R = 2) - \text{Frequency}(L/R = 6)}{\text{Frequency}(L/R = 2)} \times 100\%$.

TABLE 4.—MODE SHAPES OF LAMINATED SHELL
(L/R = 6, R/t = 33.3, AND FVR = 55%)
AS A FUNCTION OF PLY ANGLE

Ply angle, θ, deg	First frequency	Second frequency	Third frequency
$[\pm\theta]_2$	Beam mode	Torsional and radial modes	Torsional, axial, and radial modes

TABLE 5.—PERCENT DIFFERENCE IN FIRST NATURAL FREQUENCIES

Laminates	$[0]_4$	$[\pm15]_2$	$[\pm30]_2$	$[\pm45]_2$	$[\pm60]_2$	$[\pm75]_2$	$[\pm90]_2$
	Difference in natural freqencies, percent						
Thick(R/t = 20) and thin (R/t = 100)[a]	2.35	2.5	4.5	9.62	1.8	0.8	1.2
Room-temperature (T = 21 °C) and high-temperature ($T = T_g/2$)[b]	3.8	2.5	3.1	3.6	3.3	3	3.5
FVR of 65% and FVR of 55%[c]	6.06	6.05	6.1	6.3	6.2	5.4	5.8

[a]Percent difference = $\dfrac{\text{Frequency}(R/t = 20) - \text{Frequency}(R/t = 100)}{\text{Frequency}(R/t = 20)} \times 100\%$.

[b]Percent difference = $\dfrac{\text{Frequency}(T = 21\ °C) - \text{Frequency}(T = T_g/2)}{\text{Frequency}(T = 21\ °C)} \times 100\%$.

[c]Percent difference = $\dfrac{\text{Frequency}(\text{FVR} = 65\%) - \text{Frequency}(\text{FVR} = 55\%)}{\text{Frequency}(\text{FVR} = 65\%)} \times 100\%$.

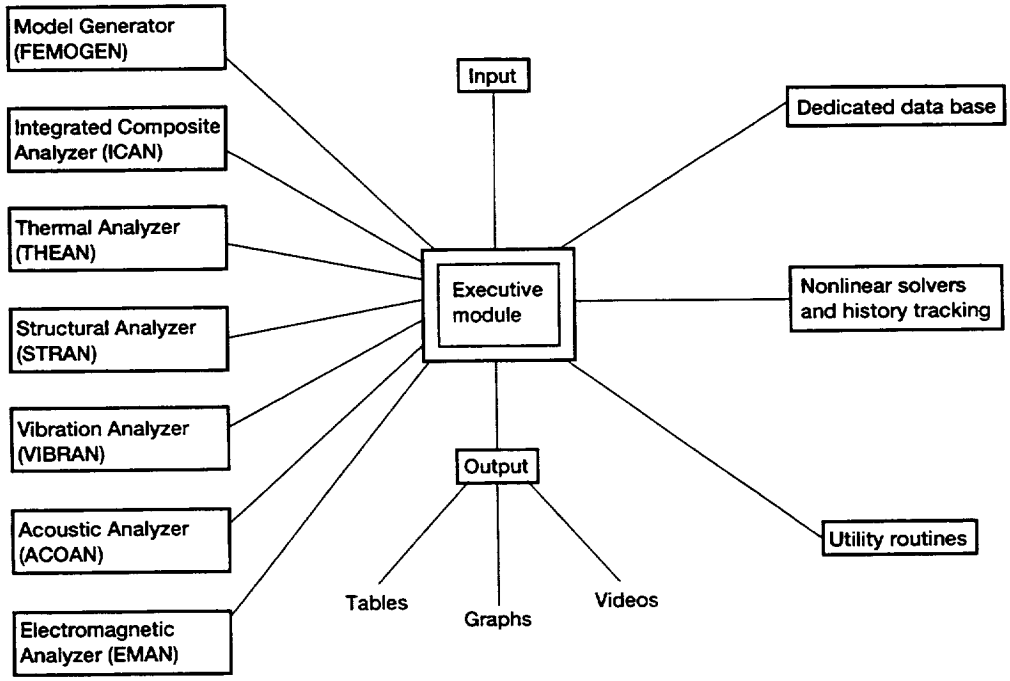

Figure 1.—CSTEM modular structure.

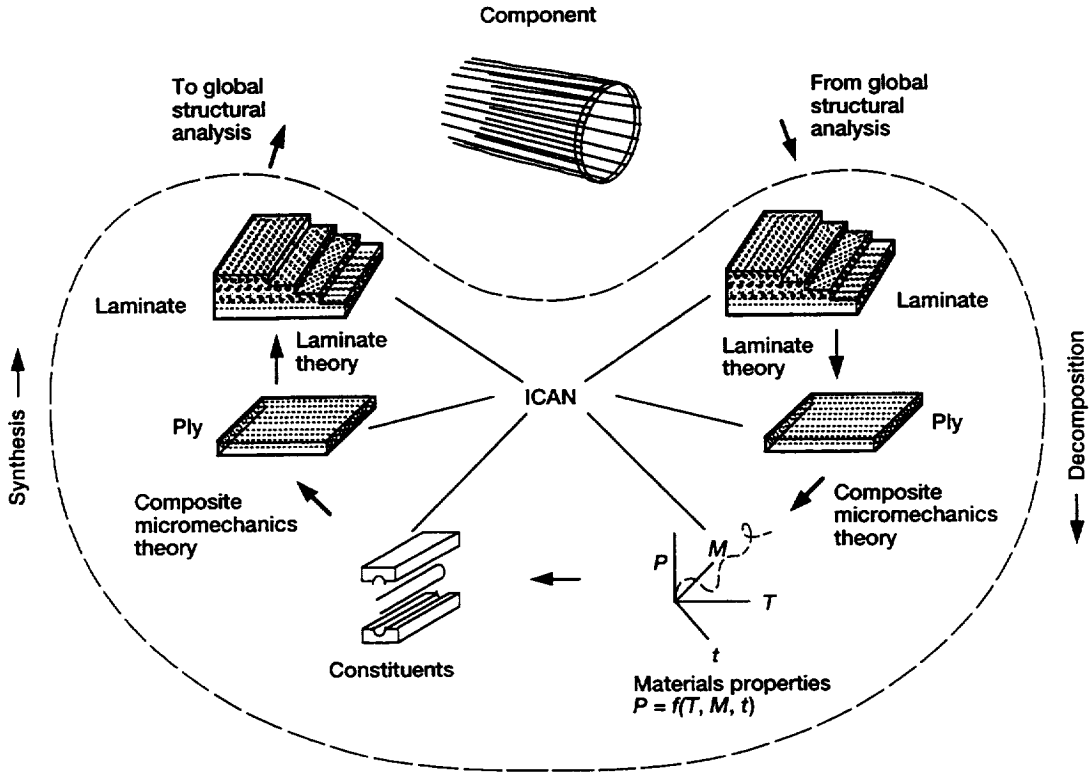

Figure 2.—Integrated Composite Analyzer (ICAN).

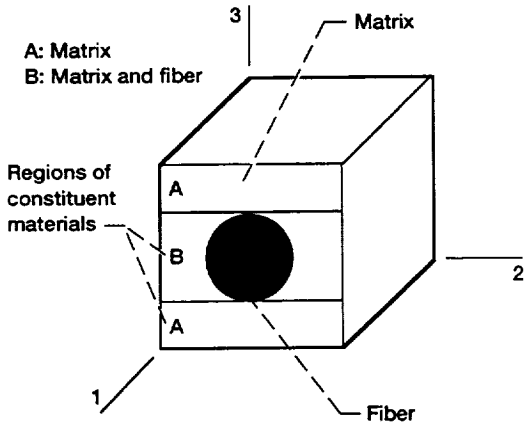

$$\frac{P_M}{P_{M0}} = \left(\frac{T_{GW} - T}{T_{GD} - T_0}\right)^{1/2}$$

$$T_{GW} = (0.005\,M^2 - 0.1M + 1)T_{GD}$$

P_M matrix property at current temperature T
P_{M0} matrix property at reference temperature T_0
T_{GW} wet glass transition temperature
T_{GD} dry glass transition temperature
M moisture

Figure 3.—Regions of constituent materials and nonlinear material characterization model.

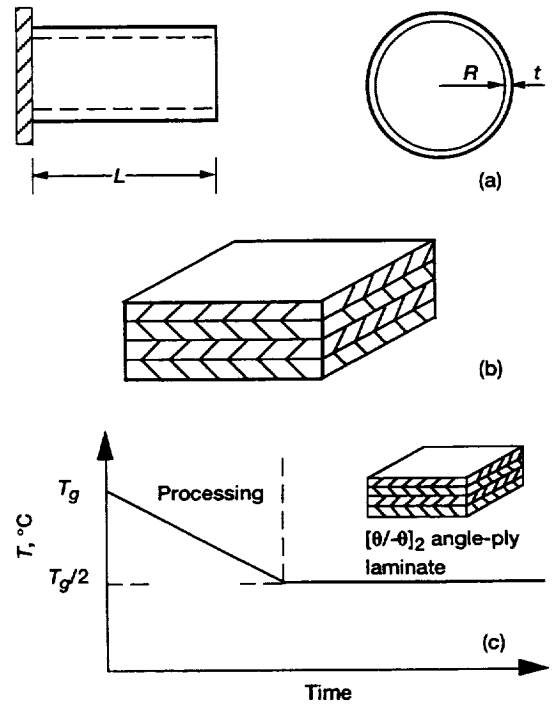

Figure 4.—Geometry, materials, and processing of laminated thin shells. (a) Geometry: $L/R = 4$; $R/t = 33.3$; $R = 25.4$ cm. (b) Materials: angle-ply laminate $[\theta/-\theta]_2$; fiber volume ratio = 55%; moisture = 2%; T300 fibers; IMHS matrix. (c) Processing. Thermal load $T_g = 215.5$ °C.

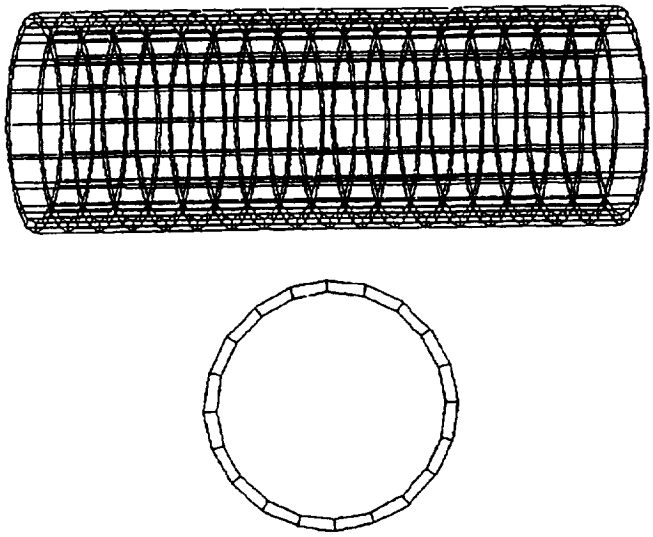

Figure 5.—Three-dimensional finite element mesh and transverse cross-sectional area of laminated thin shells.

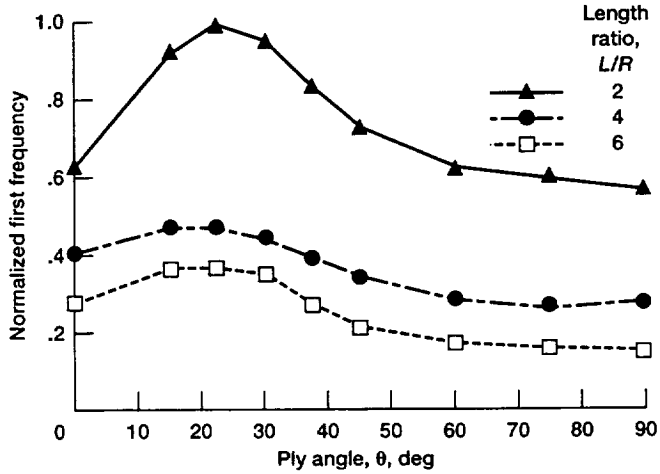

Figure 6.—Influence of shell length ratio on lowest frequency of laminated shell. R/t = 33.3; FVR = 55%; moisture = 2%; maximum normalized frequency = 554.9 Hz.

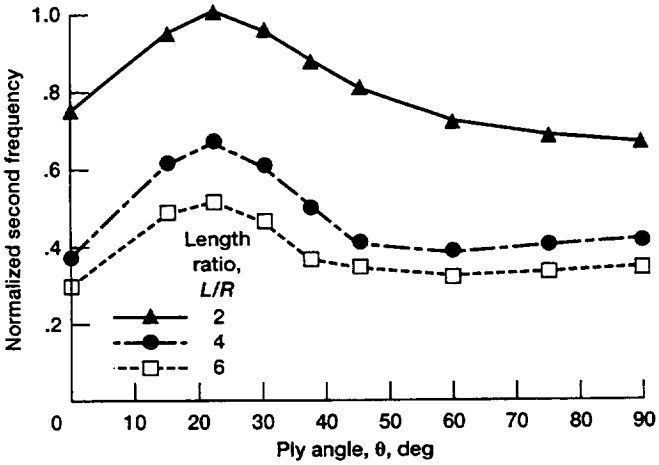

Figure 7.—Influence of shell length on second frequency of laminated shell. R/t = 33.3; FVR = 55%; moisture = 2%; maximum normalized frequency = 609.6 Hz.

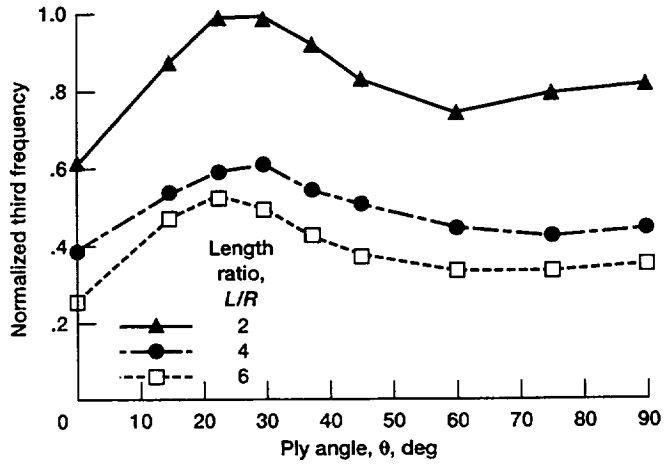

Figure 8.—Influence of shell length on third frequency of laminated shell. R/t = 33.3; FVR = 55%; moisture = 2%; maximum normalized frequency = 871.8 Hz.

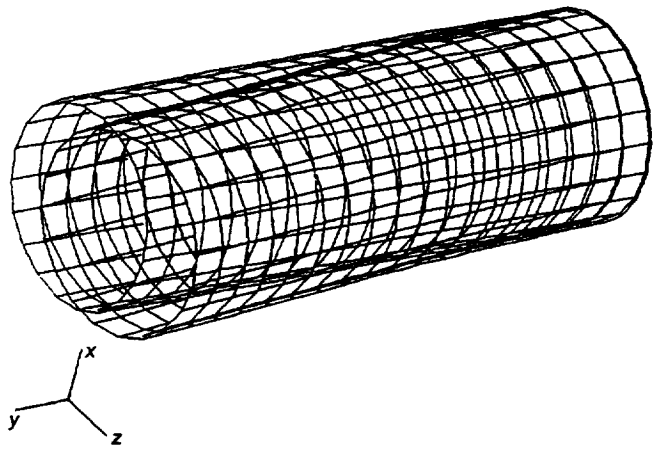

Figure 9.—First mode shape of $[\pm\theta]_2$ angle-ply laminated shell.

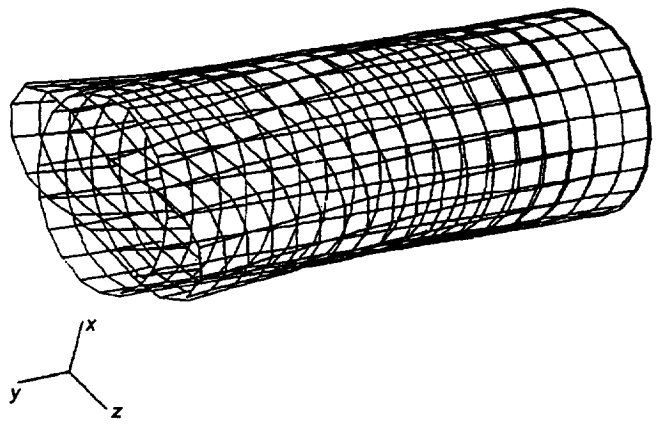

Figure 10.—Second mode shape of $[\pm\theta]_2$ angle-ply laminated shell.

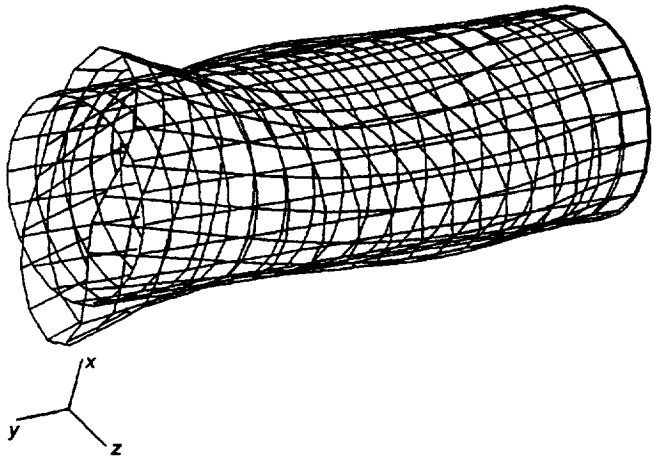

Figure 11.—Third mode shape of $[\pm\theta]_2$ angle-ply laminated shell.

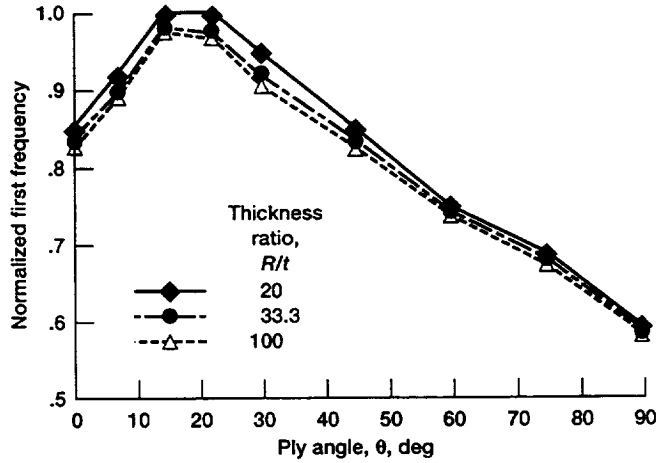

Figure 12.—Influence of laminate thickness ratio *R/t* on lowest frequency of laminated shell. *L/R* = 4; FVR = 55%; moisture = 2%; maximum normalized frequency = 264.4 Hz.

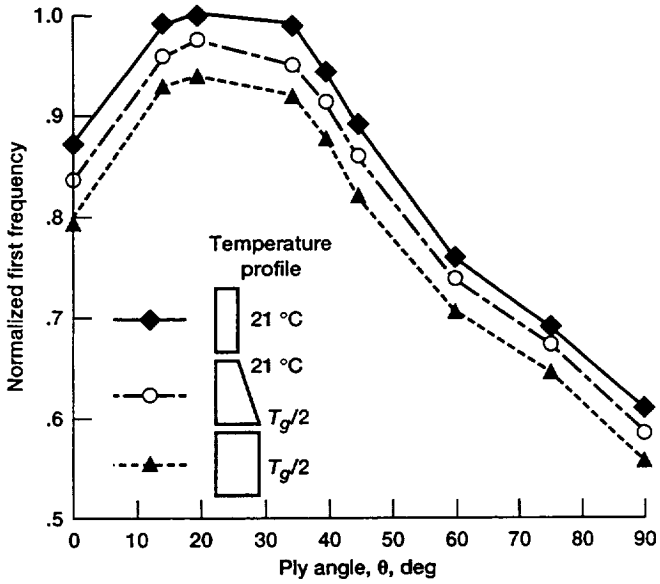

Figure 13.—Influence of temperature profile on lowest frequency of laminated shell. L/R = 4; R/t = 33.3; FVR = 55%; moisture = 2%; maximum normalized frequency = 276.8 Hz.

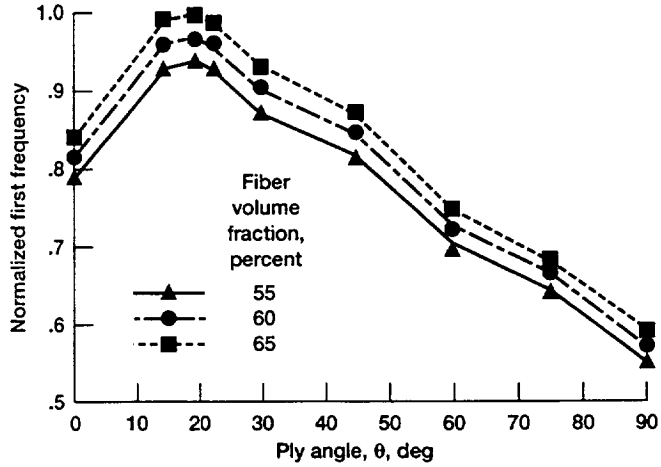

Figure 14.—Influence of fiber volume fraction on lowest frequency of laminated shell. L/R = 4; R/t = 33.3; moisture = 2%; maximum normalized frequency = 278.6 Hz.

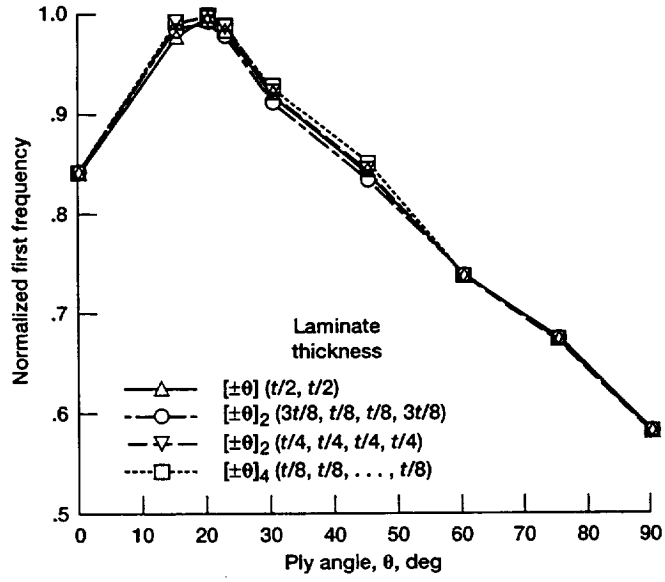

Figure 15.—Influence of laminate thickness on lowest frequency of laminated shell. L/R = 4; R/t = 33.3; FVR = 55%; moisture = 2%; maximum normalized frequency = 262.3 Hz.

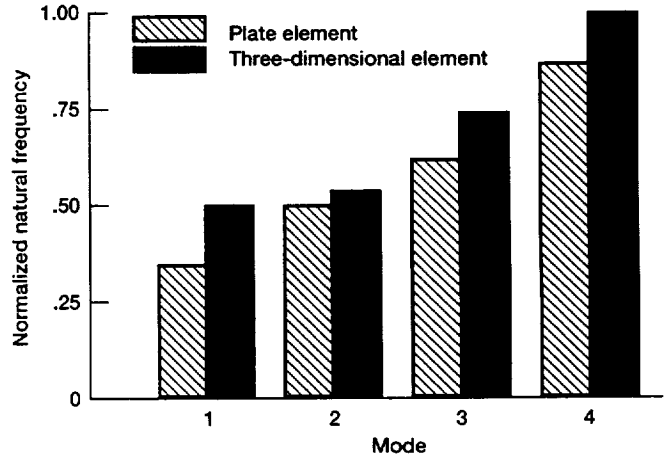

Figure 16.—Comparison of finite element analyses for eight-node, three-dimensional elements and four-node plate elements. Maximum normalized frequency = 454.16 Hz.

REPORT DOCUMENTATION PAGE

Form Approved
OMB No. 0704-0188

1. AGENCY USE ONLY (*Leave blank*)	2. REPORT DATE	3. REPORT TYPE AND DATES COVERED
	July 1993	Technical Memorandum

4. TITLE AND SUBTITLE
Laminated Thin Shell Structures Subjected to Free Vibration in a Hygrothermal Environment

5. FUNDING NUMBERS
WU-537-04-20

6. AUTHOR(S)
Pascal K. Gotsis and James D. Guptill

7. PERFORMING ORGANIZATION NAME(S) AND ADDRESS(ES)
National Aeronautics and Space Administration
Lewis Research Center
Cleveland, Ohio 44135-3191

8. PERFORMING ORGANIZATION REPORT NUMBER
E-8874

9. SPONSORING/MONITORING AGENCY NAME(S) AND ADDRESS(ES)
National Aeronautics and Space Administration
Washington, D.C. 20546-0001

10. SPONSORING/MONITORING AGENCY REPORT NUMBER
NASA TM-106600

11. SUPPLEMENTARY NOTES
Responsible person, Pascal K. Gotsis, organization code 5210, (216) 433-3331.

12a. DISTRIBUTION/AVAILABILITY STATEMENT
Unclassified - Unlimited
Subject Category 39

12b. DISTRIBUTION CODE

13. ABSTRACT (*Maximum 200 words*)
Parametric studies were performed to assess the effects of various parameters on the free-vibration behavior (natural frequencies) of $[\pm\theta]_2$ angle-ply, fiber composite, thin shell structures in a hygrothermal environment. Knowledge of the natural frequencies of structures is important in considering their response to various kinds of excitation, especially when structures and force systems are complex and when excitations are not periodic. The three-dimensional, finite element structural analysis computer code CSTEM was used in the Cray YMP computer environment. The fiber composite shell was assumed to be cylindrical and made from T300 graphite fibers embedded in an intermediate-modulus, high-strength matrix. The following parameters were investigated: the length and the laminate thickness of the shell, the fiber orientation, the fiber volume fraction, the temperature profile through the thickness of the laminate, and laminates with different ply thicknesses. The results indicate that the fiber orientation and the length of the laminated shell had significant effects on the natural frequencies. The fiber volume fraction, the laminate thickness, and the temperature profile through the shell thickness had weak effects on the natural frequencies. Finally, the laminates with different ply thicknesses had an insignificant influence on the behavior of the vibrated laminated shell. Also, a single through-the-thickness, eight-node, three-dimensional composite finite element analysis appears to be sufficient for investigating the free-vibration behavior of thin, composite, angle-ply shell structures.

14. SUBJECT TERMS
Laminated cylinders; Fiber composites; Angle-ply laminates; Composite structures; Computational simulation; Residual stresses; High temperature; Moisture; Structural analysis; Finite element analysis; Free vibration; Natural frequencies; Mode shapes

15. NUMBER OF PAGES
17

16. PRICE CODE
A03

17. SECURITY CLASSIFICATION OF REPORT	18. SECURITY CLASSIFICATION OF THIS PAGE	19. SECURITY CLASSIFICATION OF ABSTRACT	20. LIMITATION OF ABSTRACT
Unclassified	Unclassified	Unclassified	